

Rapid Search and Quantitative Analysis of Gunshot Residue Particles in the SEM

REFERENCE: Lebieczik J, Johnson DL. Rapid search and quantitative analysis of gunshot residue particles in the SEM. *J Forensic Sci* 2000;45(1):83–92.

ABSTRACT: Automated scanning electron microscopy coupled with image analysis and X-ray micro analysis was used to characterize a variety of gunshot residue (GSR) samples. More than 500 rounds of commercially available ammunition and six different types of hand guns were used in the study of 17 GSR and 19 reference specimens. The individual particle X-ray composition was determined for 12 different elements. Elemental composition of GSR particles was highly variable but consistent with compounds mixed into or associated with a barium oxide matrix. When present in a specimen, GSR could be adequately characterized with automated procedures in less than an hour by restricting analyses to features larger than 2 μm . In “clean” samples, a higher resolution particle search was required to avoid reporting false negatives. Careful control of the back scattered electron signal strength threshold, by reference to a standard, was needed to ensure both time-efficient and accurate analyses. Samples collected from non-shooting subjects, active in a physical environment which contained firearms discharge residue were seen to be easily contaminated by sub-micron GSR particles.

KEYWORDS: forensic science, scanning electron microscopy (SEM), energy dispersive X-ray analysis (EDX), gunshot residue (GSR), firearms discharge residue (FDR), gunshot residue composition, gunshot residue contamination, automatic analyses, back scattered electron (BSE) signal, imaging threshold standard

The analysis of gunshot residue (GSR) by scanning electron microscopy with energy dispersive X-ray analysis (SEM/EDX) is considered to be one of the most reliable techniques for establishing whether a person has recently fired a gun (1). It was the analytical method of choice in the pioneering studies of GSR deposition carried out by Basu et al. (2). The recent review of GSR analysis by Meng and Caddy (3) reiterates this perspective; describing the methodology as “. . . potentially superior because it characterizes individual gunshot residue particles both morphologically and elementally,” and citing homicide/assault case success rates of 79% for it. These authors point out, however, that the method is very consumptive of time and manpower. The SEM/EDX technique is somewhat expensive, in part due to the cost of the equipment consisting of an SEM, a back-scattered electron (BSE) detector and an X-ray analyzer. This equipment is very useful in a number of general forensic investigations and should not be considered as an ad-

ditional expense, except perhaps the inclusion of an image analyzer. The most significant expense is due to the time involved for a qualified microscopist to search for GSR in samples and to document the findings.

The commercial availability of computer interfaced SEM/EDX/Image Analysis systems, for more than two decades, has substantially advanced the application of the methodology to GSR analysis. The automation of these analyses (4–7) makes it possible to generate large data sets from unattended analyses, and there now exists a sufficient body of analytical experience with the technique for the American Society for Testing and Materials (ASTM) to issue a standard (8) governing GSR analysis. The present investigation was undertaken in accordance with the above mentioned ASTM standard using commercially available hardware and software. Field conditions were simulated in which more than 500 rounds of “over the counter” ammunition were fired in common handguns and samples collected by tape lift. The objectives were: 1) to demonstrate the time efficiency of automated GSR analysis, 2) to quantify the distribution of GSR particle types found under the different conditions employed, and 3) to document the extent to which GSR may be identified in ‘non-shooter’ environmental tape lift samples.

Methods

Sample Acquisition and Preparation

A number of handguns were used with commercially available ammunition to generate firearms discharge residue on the hands of subjects. Samples were produced at the Boulder, Colorado, Rifle Club range after firing a single round or multiple rounds from the following: Taurus model 94 .22 cal. revolver, Taurus model PT 99AF Semi-automatic 9 mm pistol, Ruger model SP101 .357 magnum revolver, Ruger Super Redhawk .44 magnum revolver and Para-Ordnance P14-45 Semi-automatic .45ACP cal. pistol. As the purpose was to generate GSR samples under field conditions, neither the hands nor the handguns were purposefully cleaned before the majority of tests. Some samples were taken right after the weapon was fired, while some were taken up to two hours later in our laboratory.

The conventional sample collection procedure (2,8,9) was modified to collect samples on a reduced 8 by 8 mm sample area. Because the goal was not to document the exact location of GSR particles on the hand but to reduce search and analysis time, particles needed to be collected into the smallest possible area on the sampling medium. We used SPI #5072 double-sided conductive carbon tape cut to 8 mm in length and affixed to 1/2 in. diameter aluminum pin type SEM stubs. While not evaluated by Wrobel, et al. (10), it is a featureless medium with a strong adhesive factor and little or no X-ray background.

¹ Advanced Research Instruments Corp., 2434 30th Street, Boulder, CO.

² Department of Chemistry, SUNY College of Environmental Science and Forestry, Syracuse, NY.

Received 15 Jan. 1999; and in revised form 7 May 1999; accepted 10 May 1999.

The cover on the affixed tape was removed. The tape was then lightly pressed in ten different locations on the shooting hand, starting from the trigger finger and working toward the back of the hand (Fig. 1). Light pressing was necessary in order not to crush significant GSR structures. However, enough pressure was required for effective particle transfer from the hand to the tape. Samples from each subject were collected after shooting; in most cases clean hand samples were also collected before shooting. The samples were marked for identification and immediately stored in a standard SEM sample storage box (Fig. 2). No other sample preparation was involved.

A few reference samples for this study were prepared in a different fashion. Materials like electrical solder dust, plaster and paint particles, and unburned ammunition primer particles were deposited directly on the double-sided tape/SEM stub mount. Excess material was blown off with "Aero-Duster." Some GSR sam-

ples were generated by direct deposit, firing ammunition primers into a clean plastic tube with a prepared SEM stub mounted about 30 cm below a nylon fitting machined to hold the primer cup.

Automated SEM/EDX Analyses—All samples were characterized with an ETEC Omniscan SEM fitted with a KEVEX X-ray detector and interfaced with an Advanced Research Instruments (ARI) Corp AutoSEM1 Image/X-ray analyzer and an ARI back-scattered electron detector. The X-ray detector (10 mm², 146 eV resolution) was equipped with a KEVEX linear amplifier and H.V. bias unit. A multi-channel analyzer and stage automation capabilities were an integral part of the AutoSEM1 Image/X-ray analysis system. No proprietary software specific to GSR analysis was employed. Operating conditions for the SEM utilized zero degrees tilt, a working distance of 21 mm, an accelerating voltage of 20 kV, and an X-ray acquisition of 5 s live time. The tape lift samples known to contain firearms discharge residue were analyzed at "Low resolution" defined as magnification = 44× and search pixel density = 1024 by 1024, equivalent to 2 μm pixel spacing. Many of the reference standard and background documentation samples were run at higher magnifications and search densities so as to establish a minimum feature analysis size of 0.5 μm. Analytical runs for these high resolution samples typically covered 100 fields of view, each measuring 0.5 by 0.5 mm.

Image Analyzer Threshold Settings—The heavy element composition of GSR provides excellent atomic number contrast in the back-scattered electron signal to differentiate the particles of interest from the background in tape lifts. BSE signal strength is proportional to the average atomic number of a particle being viewed in the SEM; adjusting the amplification of this signal is routinely used by microscopists in manual searches for GSR (or other high atomic number particles). In our tests, we set the image analyzer threshold for particle location to a value which was about 50% of the BSE brightness of GSR features found in reference samples. During the course of this work we adopted a simple imaging standard for routine GSR characterization. It consists of a small piece of adhesive-backed copper tape placed on the aluminum SEM stub in proximity to the carbon tape such that a line scan at low magnification crossed all three substrates. The BSE amplifier gain was set so that the signals from both the carbon tape and the copper tape were on scale; the imaging threshold was then set for the aluminum signal ($Z = 13$). A number of experiments were conducted at lower threshold settings to document the time saving of the GSR threshold (11).

X-ray Spectrometer Setup—From our own preliminary investigations and from the published reports of other researchers (12–14), firearms discharge residue (FDR) was observed to contain a variety of elements in addition to the characteristic barium, antimony and lead of GSR particles. Great variability in the elemental composition of FDR particles is to be expected because of the complex, high temperature interactions between the primer, the components of the ammunition and the particular metal alloys used in the weapon (15). We added aluminum, silicon, sulfur, chlorine, potassium, iron, nickel, copper and zinc to the list of elements routinely monitored. Except for elements lighter than sodium ($Z = 11$), which we couldn't measure, these elements largely describe the heterogeneous composition of FDR. X-ray spectrometer regions of interest (ROI) were established around the $K\alpha$ or $L\alpha$ X-ray energy centroid for these 12 elements; back-

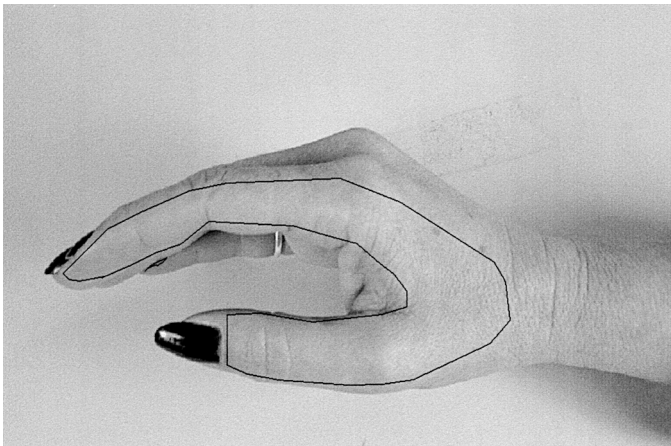


FIG. 1—The outlined area only was used to collect GSR particles. There was no attempt to locate the most dense population of GSR particles within this area.

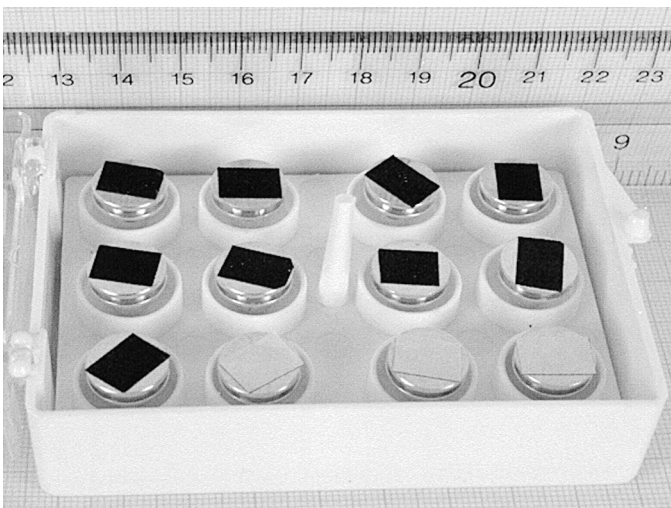


FIG. 2—Double sided tape affixed to stubs in a typical sample storage box. The upper set of samples (black) represent specimens ready for analysis. The bottom set (light color) has not been used; the cover tape is still intact.

ground was determined using the first two channels left and right of the ROI's.

GSR Classification Criteria—When the elements Pb, Ba, and Sb are the only ones for which X-ray composition is determined (4–6), GSR can be defined by the presence of all three elements or by the binary form Ba + Sb (8). Where additional elements are included, some criteria for the relative intensity of the three characteristic elements is required. We used a two step process in the data summary to classify an observation as “potential firearms discharge residue” (P-FDR): First, the presence of Pb, Ba, or Sb in the X-ray composition required net counts in those ROI's to be at least 5 times the square root of the background counts. Second, that these elements be present to the extent of at least 5% of the net X-ray count when more than one of them was present, and that the sum of Pb + Ba + Sb be at least 25% of the total net X-ray count. Particles which didn't meet these requirements were termed “Non-FDR” in origin. We defined GSR as features containing at least 5% each of Ba and Sb, with the presence of Pb optional, and with the total relative X-ray intensity of Ba + Sb + Pb > 25%. For comparison, we noted the fraction of GSR contributed by Full GSR (Ba+Sb+Pb). The remaining characteristic but not definitive P-FDR particles were subdivided into Pb-Ba (lead & barium), Pb-Sb (lead & antimony) binary classes and the three monomer classes, (Pb), (Ba), (Sb) particle types. The non-FDR (N-FDR) particle type was not classified in detail. Elemental composition of the GSR features was determined off-line by exporting the individual GSR particle observations, and utilizing SAS.

Results and Discussion

Time Efficiency of Automated Analyses

An image analyzer was used with the BSE signal to automate the search. The threshold was set to detect high atomic number particles only, capturing GSR features and ignoring most low atomic number particles. This is demonstrated in a quantitative fashion in Fig. 3, showing the effect of raising the image threshold. (The threshold is a preset grey level below which all features are ignored; above a given threshold, all particles are accepted and analyzed.) A reduction in the number of particles eligible for X-ray analysis is obvious. Setting a ‘GSR’ threshold decreased the analysis time for particles by a conservative estimate of 10 to 50 times. In Fig. 3, zero represents brightness of the substrate while 100% represents the grey level of the brightest particle. Selecting a 5% threshold in the image analyzer, just barely above the substrate, causes all particles in the field of view to be selected and analyzed. A gradual increase of the threshold results in a gradual loss of the low density particles and a more rapid analysis. Note the drastic time reduction for the analysis of a single field compared to a negligible loss of some GSR particles. The GSR features lost by raising the threshold from 5% to 50% may be considered insignificant due to their very small size and negligible contribution to the total GSR projected area fraction. By raising the threshold, the smallest particles disappear first due to a limited focus.

Another significant time saving is accomplished by limiting the feature search to larger particles. The search pixel density set by the

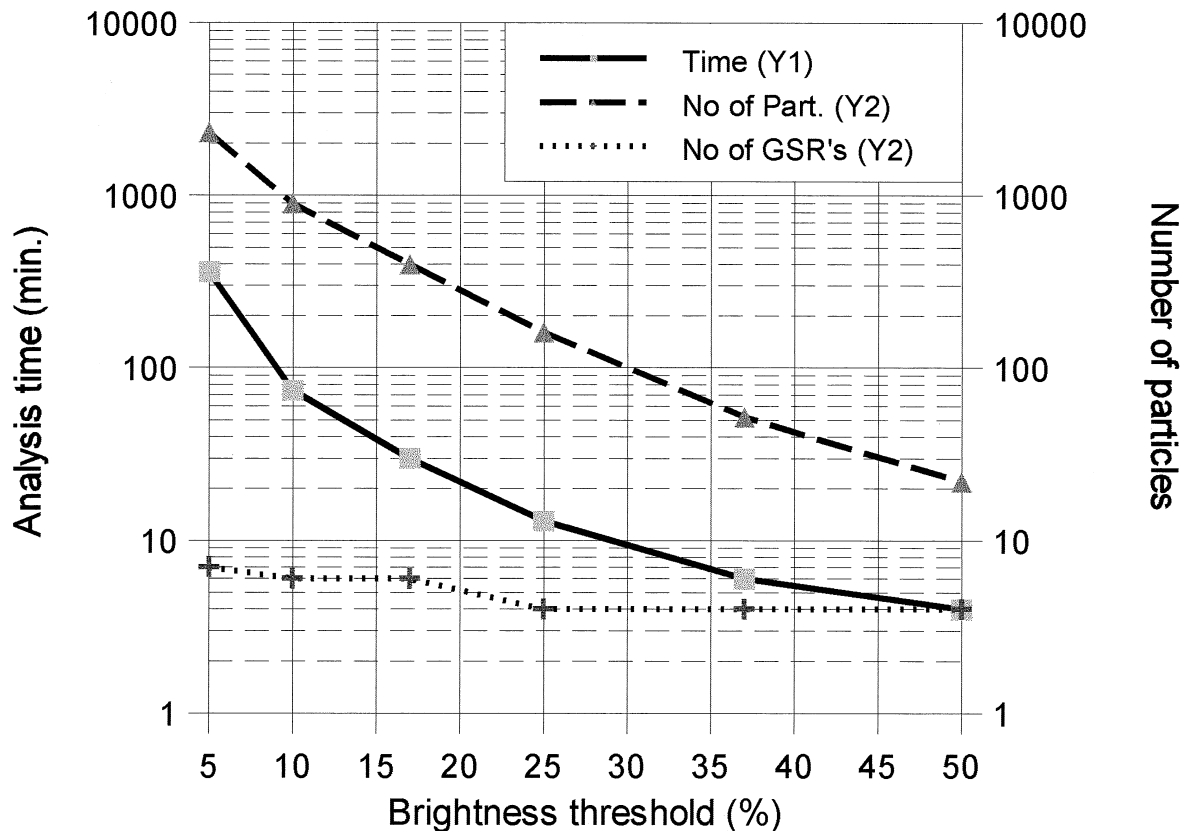


FIG. 3—A single field analysis with the image analyzer set to different thresholds (zero % represents brightness of the substrate, while 100% represents brightest particles in the field) illustrates changes in the speed of analysis. Increasing the threshold from 5% to 50% eliminates most low atomic number features but preserves the high atomic number ones. Note the drastic time reduction required for analysis from 360 min to 4 min.

image analyzer was 1024×1024 , unless otherwise indicated, resulting in $2 \mu\text{m}$ spacing for a magnification of $44\times$; this virtually ignores particles smaller than $2 \mu\text{m}$ in diameter. In some cases, particles smaller than this size are important to analyze, but for initial survey purposes, and for routine analysis of FDR samples, the $2 \mu\text{m}$ minimum size is sufficient. Figure 4 shows a comparison of high and low resolution search results for the same sample. Note that the low resolution search has covered twice the sample area in only 20% of the time (equivalent to one-tenth of analysis time for the same area), and has identified a statistically significant number of GSR features.

Table 1 shows the results of applying these instrumental conditions to the analysis of 17 different firearms discharge residue samples. Results from six common handgun types are presented, samples from the shooter's hand having been taken after discharge of 1 round and after multiple rounds. For comparison, three samples of primer discharge reference material are included. We analyzed most of the handgun samples under identical conditions, stopping after completion of 3 fields of view (about 20% of the specimen area). The samples in Table 1 designated as ".45 cal. JHP. \$" ($2 \mu\text{m}$) and ".45 cal JHP. \$" ($0.5 \mu\text{m}$) were obtained with the clean .45 cal. pistol after firing 10 rounds of 230gr JHP PMC Eldorado Star Fire ammunition. Analyses were carried out at two search resolutions as described. Results are presented by population of different classes of features, and also as a fraction of the total SEM frame area covered by those types of particles. The latter measure is expressed as ppma (parts per million area) in the data summaries. Provided the particles are of sufficiently high average atomic number to be above the GSR threshold, the ppma measure is largely insensitive to variation in threshold setting. Lowering the image analyzer threshold would increase the frame area fraction covered by lighter (non FDR) features, increasing the analysis time as well, but would have a minor influence on the GSR and PFDR area fractions.

At the BSE threshold settings we employed, the time required for characterization of GSR features in the specimens is a function of particle mass loading per unit area. This in turn varied with the

weapon and number of rounds fired. In general, the multiple rounds from higher caliber weapons resulted in a higher particle mass loading in the tape lift samples. The median percentage of particles in them classified as GSR was 11 (range 4–25%); for total area fraction, GSR had a median percentage value of 12 (range 3–37%). For samples of the CCI 350 primer only, these values were three to four times higher, being 57 (range 46–70%) and 52 (range 37–68%) respectively. When computed as GSR particles found per square millimeter of area analyzed, our results ranged from 1 to 53; by time of analysis, we found a median of 52 (range 20–169) GSR particles per hour of analysis time. Both of these results are comparable to those reported by Tillman (4).

Distribution of FDR Particle Types and the Elemental Composition of GSR

Table 2 shows the distribution of GSR and potential firearms discharge residue particle types found in the samples we analyzed. We report characteristic GSR features in Table 2, defined as previously indicated, as well as the additional binary and monomer types similar to previous investigations (2,4). It is possible that such distribution patterns of GSR and supporting particle types are characteristic of a particular weapon/ammunition combination, but a large number of replicate samples would be required under more controlled conditions in order to test that hypothesis. The most significant result shown by the data in Table 1 is the high degree to which barium seems to dominate the composition of the FDR. Unlike the results of Germani (6), we found that for the .22 cal, .357 mag, .45 cal, and 9mm weapons, the barium-antimony particle type was 50 to 80% of the GSR particle population. In multiple round tests of the .38 cal and .44 mag ammunition, the Ba-Sb particles were at least 40% of the GSR. The .38, .44, .45 and 9mm caliber weapon samples showed the Ba-Sb particle type with 1 to 3 times the full GSR area coverage. A general observation we made from our hand gun results was a larger particle size for the Ba-Sb particle type compared with the full GSR features. On the other hand, full GSR particles were the

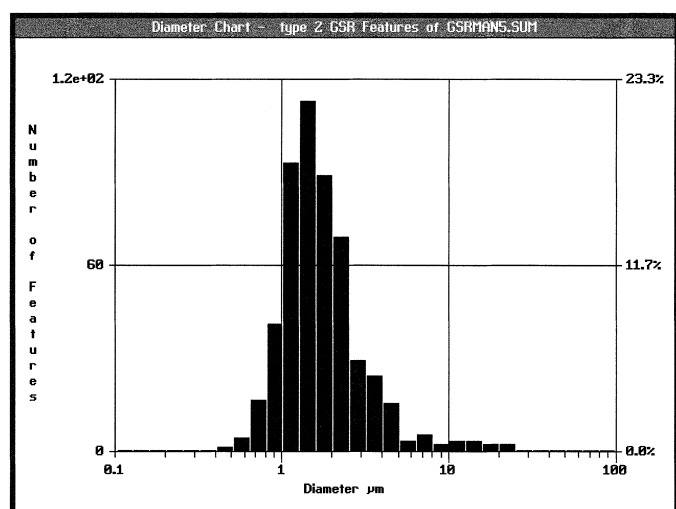


FIG. 4a—High resolution search for GSR. 45 ACP JHP Eldorado ammunition.

Search pixel spacing	$0.5 \mu\text{m}$
Total area analyzed	25 mm^2
Number of GSR particles	514
GSR area fraction	216 ppma
Total analysis time	10 h

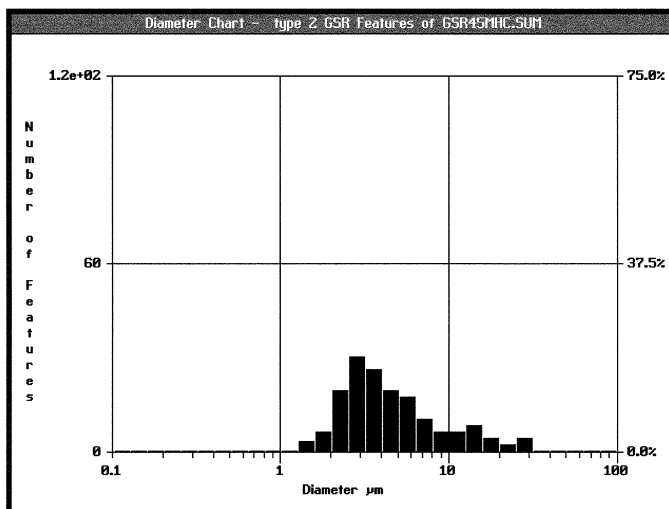


FIG. 4b—Low resolution search for GSR. Same sample as Fig. 4a.

Search pixel spacing	$2.0 \mu\text{m}$
Total area analyzed	50 mm^2
Number of GSR particles	160
GSR area fraction	166 ppma
Total analysis time	2 h

TABLE 1—Summary of GSR analyses from tests of six different weapons with single and multiple rounds.

Weapon Tested	Num. of Fields	Area Analyzed (mm ²)	Time (h)	GSR		P-FDR		N-FDR	
				Num.	Area Frac. (ppma)	Num.	Area Frac. (ppma)	Num.	Area Frac. (ppma)
.22 cal. 1 round	3	12.5	0.64	44	62	97	141	116	275
.22 cal. 80 rounds	3	12.5	8.62	194	172	634	710	2521	3073
.357 mag. 1 round	3	12.5	0.30	10	27	9	14	104	179
.357 mag. 5 rounds	3	12.5	2.53	178	120	312	158	1447	2338
.38 cal. 1 round	3	12.5	1.92	35	46	59	31	907	1887
.38 cal. 5 rounds	3	12.5	2.39	92	92	127	97	933	1234
.44 mag. 1 round	3	12.5	2.67	107	86	238	174	1166	2104
.44 mag. 12 rounds	3	12.5	5.30	486	359	1141	768	994	1497
.45 cal. 1 round	3	12.5	1.68	202	393	289	452	616	1356
.45 cal. 50 rounds	3	12.5	3.94	637	1721	608	783	1372	2194
.45 cal. JHP,\$	12	50.0	2.10	150	160	255	68	596	270
.45 cal. JHP,\$\$	100	25.0	9.88	490	152	2523	286	2815	578
9 mm 1 round	3	12.5	0.87	214	213	39	60	161	289
9 mm 30 rounds	3	12.5	4.32	176	548	181	214	1231	1604
primer CCI350a	<1	0.4	2.88	712	16,887	289	28,173	15	676
primer CCI350b	<1	0.4	1.90	560	25,578	690	16,573	63	1903
primer CCI350c	<1	0.3	1.64	300	9510	280	8141	45	467

NOTE: The number of features and the percentage of frame area covered by different particle types is given. GSR features contained at least 5% of the total net X-ray count from Ba and Sb, and may or may not have contained Pb. The PFDR category contained at least 5% of the net X-ray count from Pb, Ba, or Sb.

TABLE 2—Distribution of FDR particle types collected from test firings and from reference primer discharges. Entries refer to the number of particles of each type found regardless of their size.

Weapon Tested	Partial Firearm Discharge Residue PFDR						
	GSR Ba,Sb≥5% Pb≥0% Σ>25%	GSR (Full) Pb,Ba, Sb≥5% Σ>25%	Pb,Ba ≥5% Σ>25%	Pb,Sb ≥6% Σ>25%	Pb ≥25%	Ba 25%	Sb ≥25%
.22 cal., 1 round	44	23	18	11	36	31	1
.22 cal., 80 rounds	194	110	105	84	203	222	20
.357 mag., 1 round	10	4	1	1	4	3	0
.357 mag., 5 rounds	178	81	12	15	17	265	3
.38 cal., 1 round	35	12	0	1	1	56	1
.38 cal., 5 rounds	92	52	3	6	5	112	1
.44 mag., 1 round	107	54	2	12	9	213	2
.44 mag., 12 rounds	486	195	9	65	34	1031	2
.45 cal., 1 round	202	59	31	19	17	204	18
.45 cal., 50 rounds	637	336	93	141	111	243	20
.45 cal., JHP, \$	150	61	26	12	47	61	89
.45 cal JHP, \$\$	490	183	226	74	290	748	1185
9 mm, 1 round	214	119	5	62	15	40	3
9 mm, 30 rounds	176	36	6	35	49	57	34
Primer CCI350a	712	674	72	16	4	144	53
Primer CCI350b	560	319	41	8	9	533	99
Primer CCI350c	423	300	58	10	6	177	29

dominant type of feature found in the CCI primer tests. We don't yet know if that result is specific to the particular CCI 350 primer, or whether primer discharge residue is different in composition from that of full FDR.

The elemental composition of our FDR samples can be addressed in some detail for the 12 elements we monitored. Several issues affect the interpretation of these results: 1) The X-ray spectrometer regions of interest and associated background channels were arranged in such fashion that analysis of calcium (Ca) rich or tin (Sn) rich particle reference samples did not cause a positive in-

terference for antimony. These elements might be present in FDR, but their presence in the samples we analyzed would go undetected. 2) Our barium ROI showed a positive interference from titanium, but when tested with a titanium dioxide (TiO₂) reference sample, analyzed at the 50% GSR image analyzer threshold, we detected no barium X-ray counts. At average atomic number 12.5, TiO₂ was not detected. 3) Sulfur was corrected for its overlap with Pb M X-rays in our analyses by subtracting a constant fraction of the Pb L line net X-ray counts. We set the correction to be conservative in order to avoid reporting sulfur X-rays when they weren't actually

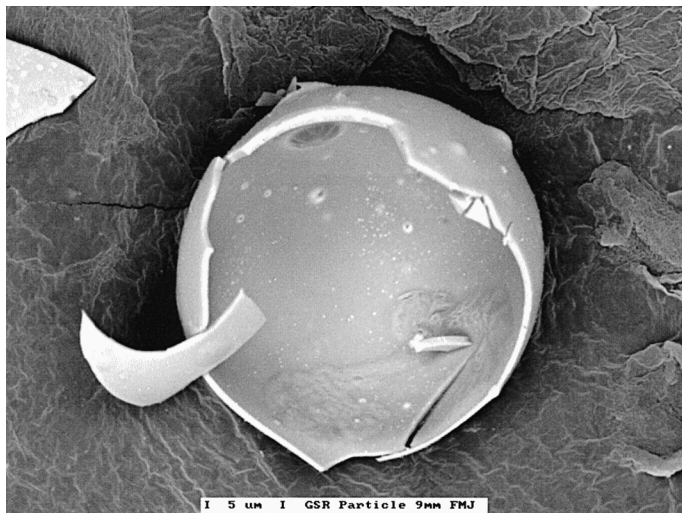


FIG. 5a—A broken GSR spheroid is revealing the inside structure or lack of it. This particle apparently broke from too high tape pressure when collected. This is the only sample that was gold coated.

Diam μm	Length μm	Width μm	W/L	X %	Y %	Area μm ²	Volume μm ³
2.99e+01	3.28e+01	2.81e+01	0.857	48.8	64.9	7.04e+02	1.41e+04
Type GSR 0Al 0Si 0S 0Cl 0K 27Sb 37Ba 0Fe 0Ni 7Cu 0Zn 6Pb							

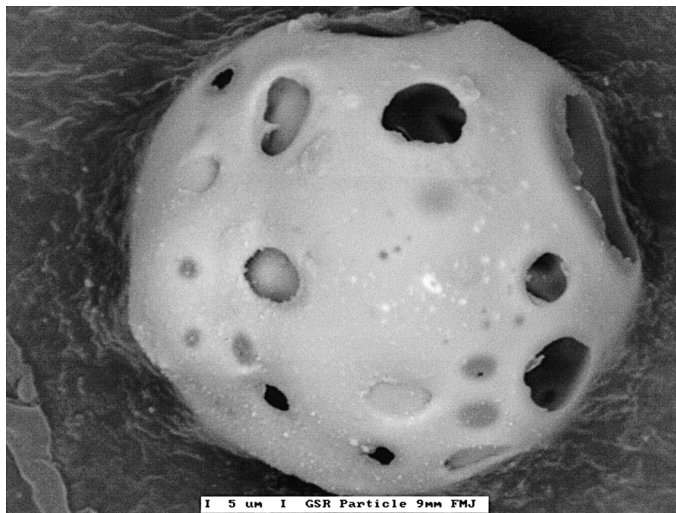


FIG. 5b—Typical GSR shape is spheroid. This one has number of holes exposing some internal structure.

Diam μm	Length μm	Width μm	W/L	X %	Y %	Area μm ²	Volume μm ³
4.79e+01	6.11e+01	4.22e+01	0.690	54.4	39.1	1.80e+03	5.75e+04
Type GSR 0Al 0Si 0S 0Cl 0K 18Sb 41Ba 0Fe 0Ni 3Cu 0Zn 6Pb							

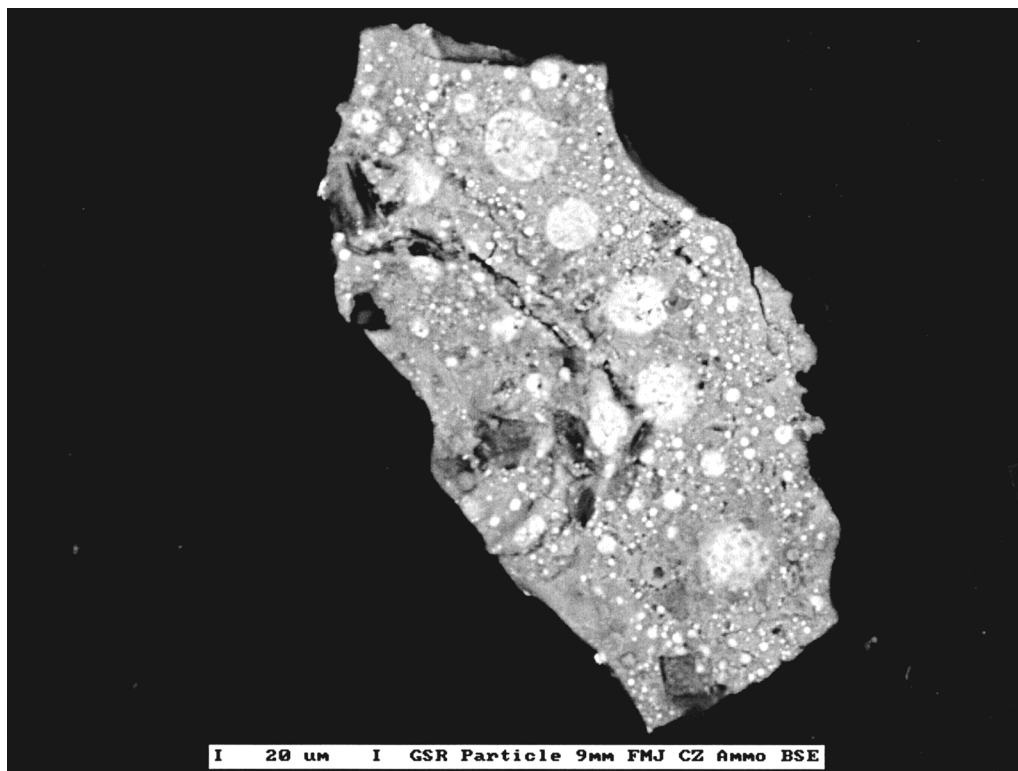


FIG. 5c—Another common shape of GSR particles is irregular shape. The bright spots are lead rich typically with some antimony.

Diam μm	Length μm	Width μm	W/L	X %	Y %	Area μm ²	Volume μm ³
6.43e+01	9.16e+01	5.03e+01	0.549	51.8	44.1	3.24e+03	1.39e+05
Type GSR 0Al 0Si 0S 0Cl 0K 22Sb 43Ba 0Fe 0Ni 4Cu 0Zn 3Pb							



FIG. 5d—Very unusual shape GSR particle. Some ammunition shows abundance of semi-spheroids connected with thin, mostly barium channel.

Diam μm	Length μm	Width μm	W/L	X %	Y %	Area μm^2	Volume μm^3
$1.63e+01$	$3.70e+01$	$2.06e+01$	0.555	1.2	58.3	$2.08e+02$	$2.26e+03$
Type GSR 0Al 0Si 0S 0Cl 0K 24Sb 30Ba 0Fe 0Ni 0Cu 0Zn 17Pb							

TABLE 3—Bulk composition of GSR particles from different weapon/ammunition tests, expressed as the relative X-ray intensity (%) contributed by the 12 elements monitored.

Elem	.22 cal LR	.357 mag	.38 Spec.	.44 mag	.45ACP Auto	.45ACP \$.45ACP \$\$	9 mm Auto	CCI-a Primer	CCI-b Primer	CCI-c Primer
Al	1 ± 3	13 ± 11	11 ± 10	15 ± 12	4 ± 5	2 ± 4	3 ± 4	4 ± 6	10 ± 9	13 ± 12	12 ± 11
Si	1 ± 2	3 ± 5	6 ± 6	3 ± 5	9 ± 9	3 ± 4	2 ± 2	8 ± 10	2 ± 3	1 ± 2	1 ± 2
S	2 ± 6	4 ± 6	11 ± 9	10 ± 11	7 ± 10	29 ± 12	27 ± 12	3 ± 7	1 ± 6	4 ± 9	4 ± 8
Cl	1 ± 4	0 ± 1	0 ± 1	0 ± 2	1 ± 3	1 ± 2	0	0 ± 3	0	0	0
K	7 ± 9	8 ± 13	7 ± 11	3 ± 5	4 ± 8	1 ± 2	0 ± 2	3 ± 7	0 ± 1	0 ± 1	0 ± 1
Sb	14 ± 8	13 ± 8	16 ± 10	15 ± 11	15 ± 9	17 ± 9	17 ± 7	15 ± 10	18 ± 11	17 ± 11	17 ± 10
Ba	31 ± 21	41 ± 18	30 ± 17	33 ± 17	37 ± 22	28 ± 16	32 ± 16	42 ± 24	33 ± 19	48 ± 21	46 ± 21
Fe	3 ± 5	2 ± 2	2 ± 3	2 ± 3	2 ± 4	3 ± 6	2 ± 5	3 ± 4	1 ± 1	1 ± 3	1 ± 3
Ni	2 ± 3	1 ± 2	1 ± 1	0 ± 1	1 ± 2	1 ± 1	0 ± 2	1 ± 2	0 ± 1	1 ± 1	0 ± 1
Cu	16 ± 12	6 ± 5	7 ± 7	11 ± 12	10 ± 11	10 ± 12	11 ± 14	10 ± 9	4 ± 4	3 ± 4	3 ± 4
Zn	3 ± 4	1 ± 1	1 ± 2	2 ± 2	2 ± 2	1 ± 2	1 ± 1	2 ± 4	0 ± 1	0 ± 1	0 ± 1
Pb	9 ± 10	7 ± 7	7 ± 6	6 ± 6	9 ± 10	4 ± 4	4 ± 4	8 ± 10	29 ± 15	12 ± 13	17 ± 16

NOTE: Uncertainties are indicated at one standard deviation. Note that oxygen and other light elements are not included. See the text for details of samples .45ACP \$(low resolution) and .45ACP \$\$ (high resolution).

present. Figure 5 shows examples of GSR features we observed in our analyses, including physical and chemical summaries. They were automatically re-located after completion of analysis from examination of the individual particle result summary. The elemental composition is indicated percentages of X-rays contributed by each of the 12 elements monitored.

Table 3 shows approximate elemental composition of the various GSR particle types we analyzed, when expressed in terms of relative X-ray intensity. (We combined the data sets for single and multiple rounds fired.) Such summaries can vary from system to system depending upon how the X-ray spectrometer regions of in-

terest are painted, how the net count corrections are applied, and how the overlap/interference corrections are administered. There are two important features of the data in Table 3: First, the GSR features are predominately composed of barium (oxide) with a nearly uniform content of antimony.

With uncertainties of one standard deviation, the coefficient of variation for barium is about 55% and that for antimony about 65%—for the other elements, the variability in composition is about twice as high. Second, the elements Pb, Al, Si, S, and Cu show substantial differences in mean value between the samples tested. Note the high sulfur content of the .45 cal. JHP samples in

Table 3. These elements, and others from different kinds of ammunition (12,14,16) could be useful in establishing a database for identification of ammunition (13), but the high degree of variability in their (X-ray) concentration indicates that large data sets will be required to account for it. In their auger spectroscopy studies of GSR, Hellmiss, et al. (16) concluded that the nucleus of most common GSR particles is barium oxide or barium aluminum oxide. Our results support this conclusion. In primer discharge samples amended with copper metal particles (atomic number 29) for consistent threshold setting, we found that the BSE signal strength from GSR features was nearly identical to that of the copper; barium oxide would have an average atomic number of 32 (very close to copper). Examination of many GSR particles, like that shown in Fig. 5c, or those described by Tassa and Zeldes (17), shows that they have a heterogeneous composition, particularly with regard to the distribution of Pb and Sb. But when considering the average X-ray makeup of a large population of GSR features, the composition is more nearly approximated by an amorphous and continuous elemental distribution across a wide range of particle sizes. We did not see significant differences in composition of GSR particles as a function of size for any of the samples we analyzed. This is illustrated by the similarity in GSR feature composition for the .45 cal. JHP samples in Table 3 run at both high and low search resolution.

Occurrence of GSR Features in "Clean" Samples

Showing that GSR is not present in a specimen requires considerably more effort than its analysis when known to be present. Despite the statistical considerations suggested by the ASTM standard, Owens (17) has concluded that in many instances nearly the entire sample needs to be searched. For our tests of "clean" sam-

ples, we searched up to 40% of the specimen area, and conducted analyses at both low (2 μm point spacing) and high (0.5 μm point spacing) search resolution conditions. We carried out 23 analyses of 20 different samples from 8 subjects, collecting samples under a variety of conditions.

Table 4 shows the results of GSR analyses of samples collected from subjects not associated with firearms discharges. As shown by subjects A-1 thru D-1 (Table 4), GSR particles are not found in samples from known "clean environments." In general, they show the absence of binary supporting particles, the Pb-Ba and Pb Sb types, though substantial numbers of Pb and Ba particles were found. Most of the Ba particles were found to be in association with sulfur—barium sulfate is commonly found in paint compositions. The low resolution searches for samples

Note the total absence of Full GSR particles in most samples. Sample D-2, where the SEM operator handled contaminated transport boxes from a firing range shows only three FGSR particles found at the high magnification only. Samples E-1 and F-1 show presence of a single, small FGSR particle each with an area fraction less than 0.1 ppm. The two subjects in those cases were at least briefly present in an area where previously three primers were discharged. The "ppma" stands for area fraction of given types of particles to the analyzed (searched) area in parts per million.

Associated with subjects A-1 and B-1 are shown for time comparisons. Note, however, that these samples at low resolution showed much smaller counts for supporting particle types. As would be expected, the high resolution search finds many more small features, but the PFDR area coverage is much more constant. This emphasizes that searches of "clean" samples requires the more time consuming analysis. In fact, specimen D-2 when analyzed at low resolution was found to be clean, whereas at high resolution,

TABLE 4—Analytical results from clean reference samples.

Sample	Res.	Area mm ²	Ana. Time h	Total Num.	FGSR Num.	Ba+ Sb Num.	Ba+ Pb Num.	Pb+ Sb Num.	Pb Num.	Ba Num.	Sb Num.	FGSR Area ppma	PFDR Area ppma
Electronics Tech. Sample #A-1	low	12.5	2.9	2645	0	0	0	0	2	26	0	0.0	19.0
Electronics Tech. Sample #A-1	high	25.0	4.6	519	0	0	0	0	181	22	1	0.0	26.4
Office Worker Sample #B-1	low	38.0	1.1	519	0	0	0	0	0	6	0	0.0	1.8
Office Worker Sample #B-1	high	25.0	4.1	230	0	0	0	0	6	17	1	0.0	0.8
Construct. Worker Sample #C-1	high	25.0	6.6	1720	0	0	1	1	10	70	1	0.0	6.9
SEM Operator Sample #D-1	high	25.0	5.8	2595	0	0	1	0	25	46	0	0.0	8.4
SEM Operator Sample #D-2	low	38.0	0.4	110	0	0	1	1	5	4	2	0.0	2.5
SEM Operator Sample #D-2	high	25.0	5.5	1962	3	2	8	10	79	117	19	0.3	12.4
Office Worker Sample #E-1	high	25.0	4.3	494	1	0	1	0	13	24	0	<0.1	1.4
Electronics Prod. Work. Samp. #F-1	high	25.0	27.8	15021	1	0	20	7	7557	197	175	<0.1	580.7
Blank Tape #1	high	25.0	3.9	15	0	0	0	0	1	2	0	0.0	0.1
Blank Tape #2	high	25.0	3.9	7	0	0	0	0	1	4	0	0.0	0.2

FGSR = Full GSR, PFDR = Potential Firearm Discharge Residue.

Note the total absence of Full GSR particles in most samples. Sample D-2, where the SEM operator handled contaminated transport boxes from firing range shows only three FGSR particles found at the high magnification only. Samples E-1 and F-1 show presence of a single, small FGSR particle each with an area fraction less than 0.1 ppm. The two subjects in those cases were at least briefly present in an area where previously three primers were discharged. The "ppma" stands for area fraction of given type of particles to the analyzed (searched) area in parts per million.

TABLE 5—Results of analyses of reference samples.

Sample	Res	Sample Area mm ²	Analysis Time h	Total Num.	FGSR Num.	BaSb Num.	PbBa Num.	PbSb Num.	Pb Num.	Ba Num.	Sb Num.	FGSR Area ppm	PFDR Area ppm
C-2	high	25.0	9.9	4263	70	91	78	27	63	263	24	10.2	39.7
G-1	low	12.5	2.5	1821	0	0	1	0	3	32	0	0.0	38.0
G-2	low	12.5	1.2	856	0	0	0	0	1	52	0	0.0	108.1
G-3	low	34.5	25.3	10698	1	6	0	0	3	123	2	2.2	33.2
G-3	high	25.0	8.2	4421	27	20	26	23	29	1055	13	4.2	35.5
G-4	high	25.0	9.3	3557	49	40	34	46	153	191	22	4.1	32.1
H-1	high	25.0	5.0	566	3	0	1	0	13	24	0	0.2	3.9
G-5	high	25.0	4.5	387	32	35	7	6	32	18	8	6.7	3.3
G-6	low	12.5	0.2	114	4	5	1	0	2	7	1	5.8	14.8
G-7	low	12.5	1.6	527	28	25	2	14	17	17	11	42.0	39.8
G-8	high	25.0	8.4	2610	3	5	4	10	28	65	10	1.0	10.7

PFDR = Potential Firearms Discharge Residue.

FGSR = Full GSR.

C-2 Construction worker at range samples after set up.

G-1 Subject sampled at range before set up.

G-2 Same as G-1, but different date.

G-3 Sampled at the range before set up, different date.

G-4 Subject carried and unpacked equipment bag, set up session; sampled before shooting.

H-1 Subject at range, not involved in session set up.

G-5 Subject sampled 2 h after session of reloading 9 mm ammunition; no weapons discharged.

G-6 Subject sampled 4 h after shooting range session.

G-7 Subject sampled 1 h after shooting range session and after normal hand washing.

G-8 Same as G-7, but different date and after vigorous hand washing.

GSR particles were identified. Samples E-1 and F-1 also showed the presence of a single GSR feature, but it is likely that these represent contamination from handling; all of the GSR features found in samples D-2, E-1 and F-1 were smaller than 1 μm in diameter. The blank samples did not show GSR particles though atmospheric deposition did result in a few high atomic number features.

Further evidence of environmental contamination is shown by the results in Table 5. Sample C-2 was taken from the same individual as sample C-1 (Table 4), and on the same day, but after set up activities at the firing range. Samples G-1 and G-2 were sampled at the firing range before set up. These analyses were under analytical conditions comparable to those for the known FDR samples (Table 3). Sample G-3 was similar in nature to G-1 and G-2, but its analysis was carried out at both low and high search resolution. The latter analysis showed considerable GSR. Samples G-4 and H-1 were collected on the same date from two subjects prior to shooting; the subject for G-4 was actively involved in set up activities, while H-1 was merely present in the same environment. The presence of GSR and supporting particles in the latter sample could only have been the result of environmental contamination. Sample G-5 demonstrates such contamination from another non-shooting firearms related activity. Samples G-6 through G-8 show the persistence of GSR particles with time and demonstrate that it is possible to find them even after the subjects had washed their hands.

The study by Gialamas et al. (18) showed a very low incidence of GSR on the hands of non-shooting police officers, and their samples were collected in a "clean" physical environment similar to that of our Table 4 results. However, for the 43 samples submitted to automated SEM/EDX analysis for GSR, they reported only a total of 260 particles characterized. This is much lower than even our cleanest samples where Ba particles alone occurred to the extent of 20 to 70 per sample. One possible explanation for the differences is the BSE threshold used. If Gialamas et al., had used the GSR threshold of Germani (11), equivalent to atomic number 30, most of the GSR features in the samples would have been missed.

Tables 4 and 5 show some examples of high resolution GSR searches requiring more than 8 h to complete. The blank analyses from Table 4 show that with our instrumentation, approximately 4 h is needed to search 100 fields of view with dimensions 0.5×0.5 mm using a search density of $0.5 \mu\text{m}$. The longer times mentioned above for samples C-2, G-3, and G-4 result primarily from analysis with an imaging threshold set too low; that is, large numbers of low atomic number non-FDR particles were analyzed. When GSR features are present in high abundance, establishing a time efficient image threshold for analysis is a straight forward process; 50% of the maximum BSE signal brightness will give an average atomic number of about 15 and avoid characterization carbonates, silicates and alumino-silicates, and titanium dioxide. When such bright features are absent, reference to an imaging standard is useful to reduce analysis time. In the unusual event that the sample is dominated by very high average atomic number features other than GSR, as in sample F-1 (Table 4) dominated by solder fume particles, use of the imaging standard prevents establishing an image analysis threshold too high for accurate GSR determination. The 57 to 43% Pb/Sn solder has an average atomic number of 68; setting a 50% threshold in this case would eliminate many GSR particles.

Conclusions

In the SEM X-ray micro analysis of firearms discharge residue, the presence of barium and antimony, with lead as optional, is sufficient for the elemental identification of a GSR particle. In this work, the results are based on this definition of GSR; the lead was found missing in many obvious GSR features. As the chemical composition of ammunition moves towards replacement of lead, it is important to recognize this broader definition of gunshot residue.

The elemental composition of GSR is dominated by barium; its BSE signal strength is consistent with barium oxide as the major component. The elemental composition of GSR features is approximated by a solid solution of compounds, resulting in a more nearly

continuous distribution of composition rather than an assemblage of discrete chemical particle types. Little composition variation is observed as a function of particle size.

These compositional characteristics are advantageous to the automated SEM/EDX analysis of samples for GSR. Setting a BSE signal strength threshold equivalent to atomic number 15 causes the analysis to miss non-FDR particles in the samples which significantly decreases analysis time. Further time saving is accomplished by limiting the search point density to features larger than 2 μm . Under such conditions, when GSR particles are present in the sample, statistically significant populations of them can be characterized in less than an hour.

The gunshot residue particle count or number is an insufficient description of GSR presence. Usually it is complemented by average size, or size distribution. The area fraction number, ppm, accurately combines both measures. It is the closest expression of actual GSR concentration by area of sample analysis.

Analytical conditions for avoiding false negative results are more stringent. GSR particles which remain on a subject's hands several hours after firing a weapon, or after washing of the hands, are significantly depleted in the larger size fractions. Analyses must be carried out at higher search resolutions, and to be time efficient, the BSE signal strength threshold must be carefully adjusted; reference to an imaging standard is recommended.

Samples collected in a physical environment where GSR particles have been produced are easily contaminated by sub-micron firearms discharge residue. Walking around at a firing range, setting up equipment there, or reloading spent shell casings are examples of activities which have resulted in the identification of GSR from reference (non-shooting) samples.

Acknowledgments

The authors are grateful to the Boulder Rifle Club for providing the shooting facilities.

References

1. DI Maio VIM. Gunshot wounds. CRC Press 199, 1993.
2. Basu S, Boone Jr CE, Denim Jr DJ, Musgoi RA. Fundamental studies of gunshot residue deposition by glue lift. *J Forensic Sci* 1997;42(4): 571–81.
3. Meng HH, Caddy B. Gunshot residue analysis—a review. *J Forensic Sci* 1997;42(4):553–70.

4. Tillman WL. Automated gunshot residue particle search and characterization. *J Forensic Sci* 1987;32(1):62–71.
5. White RS, Owens AD. Automation of gunshot residue detection and analysis by scanning electron microscopy/energy dispersive X-ray analysis. *J Forensic Sci* 1987;32(6):1595–603.
6. Germani MS. Evaluation of instrumental parameters for automated scanning electron microscopy gunshot residue analysis. *J Forensic Sci* 1991;36(2):331–42.
7. Zeichner A, Lenin N. Casework experience of GSR detection in Israel, on samples from hands, hair, clothing using an autosearch SEM/EDX system. *J Forensic Sci* 1995;40(6):1082–5.
8. Designation E 1588–95, Standard guide for gunshot residue analysis by scanning electron microscopy/energy-dispersive spectroscopy. Annual Book of ASTM Standards, American Society of Testing and Materials. West Conshohocken, PA, 1995.
9. Basu S, Ferriss S. A refined collection technique for rapid search of gunshot residue particles in the SEM. *Scanning Electron Microscopy* 1980;1:375–84.
10. Wrobel HA, Millar JJ, Kijek M. Comparison of properties adhesive tapes, tabs, and liquids used for the collection of gunshot residue and other trace materials for SEM analysis. *J Forensic Sci* 1998;43(1): 178–81.
11. Germani MS. Application of automated electron microscopy to individual particle analysis. *American Laboratory*, 1993;17–24.
12. Harris A. Analysis of primer residue from CCI Blazer lead free ammunition by scanning electron microscopy/energy dispersive X-ray. *J Forensic Sci* 1995;40(1):27–30.
13. Wrobel HA, Millar JJ, Kijek M. Identification of ammunition from gunshot residues and other cartridge related materials—a preliminary model using .22 caliber rimfire ammunition. *J Forensic Sci* 1998;43(2):324–8.
14. Miyauchi H, Kumihashi M, Shibayama T. The contribution of trace elements from smokeless powder to post firing residues. *J Forensic Sci* 1998;43(1):90–6.
15. Zichner A, Schecter B, Brener R. Antimony enrichment on the bullets' surfaces and the possibility of finding it in gunshot residue (GSR) of the ammunition having antimony-free primers. *J Forensic Sci* 1998;43 (3):493–501.
16. Hellmiss G, Lichtenberg W, Weiss M. Investigation of gunshot residues by means of Auger electron spectroscopy. *J Forensic Sci* 1987;32(3): 747–60.
17. Owens AD. A re-evaluation of the Aerospace Corporation final report on particle analysis—when to stop searching for gunshot residue (GSR)? *J Forensic Sci* 1990;35(3):698–705.
18. Gialamas DM, Rhodes EF, Crim D, Sugarman LA. Officers, their weapons and their hands: an empirical study of GSR on the hands of non-shooting police officers. *J Forensic Sci* 1995;40(6):1086–9.

Additional information and reprint requests:

Jozef Lebedzik, Ph.D.
5151 Ward Rd.
Suite #1
Wheat Ridge, CO 80033